Article

Smartphone screen integrated optical breathalyzer

Jerome Lapointe[1,*], Hélène-Sarah Becotte-Boutin[2], Stéphane Gagnon[1], Simon Levasseur[1], Philippe Labranche[1], Marc D'Auteuil[1], Manel Abdellatif[3], Ming-Jun Li[4] and Réal Vallée[1]

[1] Centre d'Optique, Photonique et Laser (COPL), 2375 Rue de la Terrasse, Université Laval, G1V 0A6, Québec (Qc), Canada; rvallee@copl.ulaval.ca (R.V.); stephan.gagnon@copl.ulaval.ca (S.G.); simon.levasseur@copl.ulaval.ca (S.L.); philippe.labranche.1@ulaval.ca (P.L.); marc.dauteuil@copl.ulaval.ca (M.D.);

[2] Groupe de Recherche Indépendant en Science des Données et des Décisions (GRISDD), 633 Av. Des Oblats, G1N 1W1, Québec (Qc), Canada; helene@grisdd.com (H.B.)

[3] Polytechnique Montreal, C.P. 6079, Succ. Centre-ville, Montreal, H3C 3A7, Canada; manel.abdellatif@gmail.com (M.A.)

[4] Corning Incorporated, SP-AR-02-5, Corning, NY 14831, USA; LiM@Corning.com (M.L.)

* Correspondence: jerome.lapointe@copl.ulaval.ca

Abstract: One third of fatal car accidents and so much tragedies are due to alcohol abuse. These sad numbers could be mitigated if everyone had access to a breathalyzer anytime and anywhere. Having a breathalyzer built into a phone or a wearable could be the way to get around the reluctance to carry a separate device. Towards this goal, we propose an inexpensive breathalyzer that could be integrated in the screen of mobile devices. Our technology is based on the evaporation rate of the fog produced by the breath on the phone screen, which increases as a function of the breath alcohol content. The device simply uses a photodiode placed on the side of the screen to measure the signature of the scattered light intensity from the phone display that is guided through the stress layer of the Gorilla glass screen. A part of the display light is coupled to the stress layer via the evanescent field induced at the edge of the breath microdroplets. We demonstrate that the intensity signature measured at the detector can be linked to the blood alcohol content. We fabricated a prototype in a smartphone case powered by the phone's battery, controlled by an application software installed in the smartphone and tested it in real-world environments. Limitations and future work toward a fully operational device are discussed.

Keywords: breathalyzer; wearable; sensors; breath analysis device; health; mobile screen; alcohol; ethanol; smartphone; multimedia screen

1. Introduction

Extensive research has been conducted on the topic of portable breathalyzer [1-8]. Thousands of articles and patents have been published about the consumption of alcohol in the last years and the numbers are increasing exponentially. The scale of the scientific investments is a revealing response to the numerous tragic accidents linked to alcohol abuse. At least one impaired driving incident per 500 people is reported annually and about 1 over 3 fatally injured drivers in North America had a Blood Alcohol Content (BAC) in excess of 0.08% in the last decades [9,10]. This represents over 10,000 deaths per year linked to impaired driving in the United States alone. Accordingly, alcohol abuse is understandably an important social concern.

In order to know if they can drive, people mostly rely on their symptoms or the number of drinks they took. The problem with this method is that first, the BAC is influenced by the amount of food, the sex and the body mass of a person [11]. Second, the intensity of the symptoms (nausea, slurred speech, lack of coordination) varies from person to person depending of their drinking habits [12]. Therefore, two individuals with the same BAC can have a very different perception of their level of intoxication. Besides using a breathalyzer or blood sampling, there is no heuristic or approximation that can help someone figuring out by themselves whether they are legally allowed to drive or not.

As of now, two of the most effective measures that prevent drinking and driving-related fatalities and injuries, are roadblocks and ignition interlock devices [13]. One could think that the surge of availability of portable breathalyzer could help improve the situation. Unfortunately, this hypothesis has been proven wrong. Their use is not popular among the population as people are simply not interested in carrying such a device [14]. On the other side, smartphones and wearables are widely used. Having a breathalyzer built into a phone or a wearable could be the way to get around the reluctance to carry a separate device and have a real impact on impaired driving or other alcohol related incidents.

For these reasons, any milestone toward an inexpensive breathalyzer built into a phone or any wearable is of great importance. In this article, we propose a technology that could meet this demand. Our approach only requires a photodiode placed on the side of the glass screen of any mobile device such as smartphones or smartwatches. The photodiode measures an optical signature of the light from the display that varies as a function of the evaporation rate of the water vapor when a user breathes on the screen. The evaporation rate varies for different BAC. The principle of our technology is first explained. Then, results using our prototype in laboratory and in real-world environment are presented. Finally, the ambient and breathing conditions that affect the BAC measurements are studied and future work to increase the breathalyzer precision is discussed.

2. Breathalyzer principle

Our optical breathalyzer is based on the evaporation rate of water vapor from the breath. As shown in Fig. 1 (a), when a person fogs a glass window (e.g. a smartphone screen) with his breath, thousands of microdroplets are formed on the glass surface. The evaporation rate of the microdroplets depends on the breath alcohol concentration [15], which is linked to the BAC [1-8]. On a dry screen, the light from the smartphone display crosses the glass screen and only a small part is reflected (Fresnel reflection) back to the display, see Fig. 1 (b). As shown in Fig. 1 (c), when a droplet is formed on the glass screen, part of the light is guided towards the edge of the glass screen (as light does in an optical fiber). Indeed, the edge of the droplet allows a strong oblique reflection (total internal reflection) which can be coupled into the planar waveguide formed by the dense anti-scratch stress layer. This stress layer is found in multimedia device screens made of toughened glass such as Corning Gorilla® and AGC Inc. Dragontrail® glasses. Note that ray optics is insufficient to treat this coupling behavior with the planar waveguide. Using wave optics permits us to see that light sources near the waveguide interface can interact with the evanescent field tails of the waveguide modes and hence can transfer some of their power to them [16,17]. Therefore, only the light reflected from the very edge of the water droplets can be efficiently coupled to the planar waveguide at the surface of the glass screen. This is the key principle of our optical breathalyzer. Note that recent work has demonstrated the integration of invisible photonic devices and sensors in smartphone screens using laser writing of optical waveguides [18-21]. However, the complexity of laser writing added to the use of an external light source increase the cost and the mass production complexity. In our approach, the use of the display light already present and the stress layer planar waveguide simplify greatly the integration into smartphones.

Fig. 1 (d) is a photograph of the side edge of the glass screen when the phone displays a white image at maximum brightness while the glass screen is fogged by the breath. The illuminated line comes from the microdroplets since the image is entirely dark when there are no microdroplets (i.e., when the screen is dry). Using a photodiode placed at the edge of the glass screen, the light intensity curve as a function of time can be linked to the evaporation rate of the microdroplets. The aim of this article is to demonstrate that this optical principle can be used to monitor BAC by breathing on a smartphone screen.

Preprints (www.preprints.org) | NOT PEER-REVIEWED | Posted: 19 April 2021 doi:10.20944/preprints202104.0502.v1

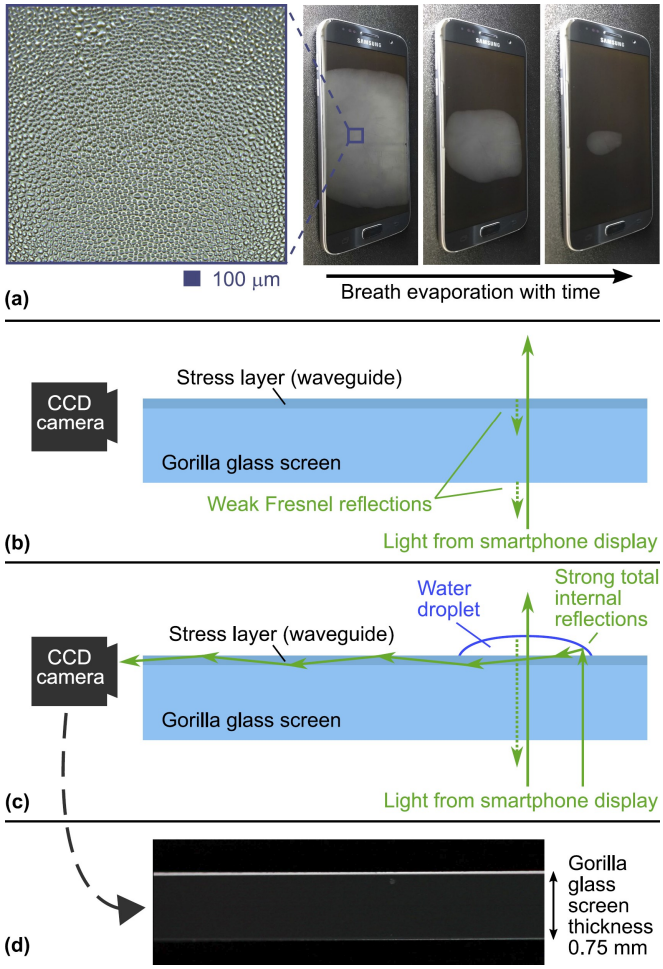

Figure 1. The optical breathalyzer principle. (a) Evaporation of the microdroplets when a person breathes on a glass screen. The inset is a zoom on the microdroplets. (b) The light from the smartphone display is not coupled to the planar waveguide on the surface of the glass screen. (c) With water droplets on the glass screen, the light from smartphone display is coupled to the planar waveguide, due to the strong oblique reflections at the edge of the droplets and is guided to the side of the screen. (d) Photograph of the guided light in (c) using a CCD camera and a 10× objective lens.

3. Breathalyzer prototype

At this stage, the technology is not fully integrated in the smartphone, for obvious reasons. Nevertheless, since the only required component that is not already part of a smartphone is a photodiode placed on the edge of the screen, we believe that the technology could be easily integrated. As shown in Fig. 2 (a), our prototype acts as a protecting case, which is also ubiquitous among the smartphone users. It is fabricated using a Corning Gorilla® glass screen, as found on most smartphone. A 7.5 cm × 13.5 cm piece has been cut to fit over a standard smartphone. This glass screen is placed on the top of the actual smartphone screen and does not affect its functions. The side edge of the Gorilla glass screen was polished to optical quality (down to a 0.5 µm grid) prior the photodiode installation. Fig. 2 (b) schematizes how the photodiode has been installed on the side of the glass screen to optimize the collection of the light from the microdroplets and minimize the noise.

Preprints (www.preprints.org) | NOT PEER-REVIEWED | Posted: 19 April 2021 doi:10.20944/preprints202104.0502.v1

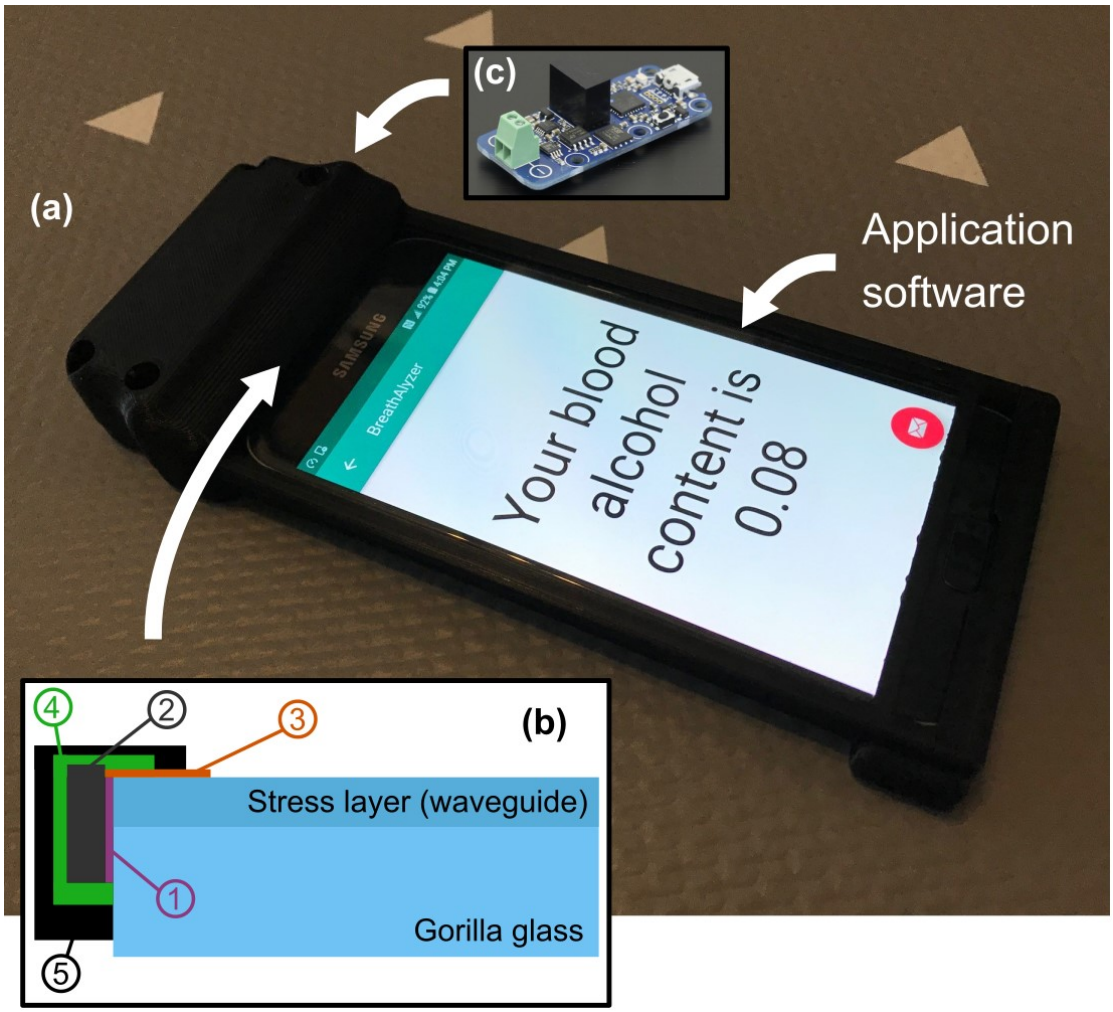

Figure 2. The optical breathalyzer prototype. (a) Photograph of our prototype. (b) Scheme of the photodiode installation on the side of the glass screen. (c) The electronics.

First, a UV curing glue (Norland Optical Adhesive NOA63) with a refractive index that matches that of the glass to minimize the Fresnel reflection is used (1) to stick the photodiode (2). The silicon photodiode used (Advanced Photonix PDB-C612-2) has a thickness of 360 µm with an active area of 3.91 mm × 17.55 mm. Then, a thin layer of UV curing glue with a low refractive index n = 1.4 is applied on the glass surface, as shown in Fig. 2 (b) (3), to maintain the guiding property of the stress layer. A strong epoxy glue is then applied (4), covering the entire photodiode, to increase its shock resistance. Finally, a very opaque black paint is applied (5) to minimize the noise from the ambient light. To measure the voltage generated by the photodiode, a voltmeter chip (2 × 4.5 × 1.16 cm^3) from Yoctopuce (Yocto-milliVolt-Rx) is connected to the photodiode and the smartphone USB port (see Fig. 2 (c)). Finally, an application software is programmed to guide the user, run the test and display the BAC results. The entire prototype uses the phone's battery to operate.

4. Results and discussion

4.1. Laboratory tests

Before testing our prototype in real-world environment, tests have been conducted in laboratory in controlled environment (class 100,000 clean room). A volunteer was asked to breathe several times on the prototype for about 2 seconds under the same conditions to the best of his ability, before and after drinking alcohol. To compare our prototype with an accurate BAC value of

Preprints (www.preprints.org) | NOT PEER-REVIEWED | Posted: 19 April 2021 doi:10.20944/preprints202104.0502.v1

the volunteer, four breath tests (two just before and two just after using our prototype) were carried out using a breathalyzer (model APC-90 from Alco Prevention Canada Inc.) approved by the U.S. Food and Drug Administration (FDA). Fig. 3 (a) shows typical curves of the light intensity as a function of the time measured by our prototype for different BACs. The light intensity increases while the volunteer is breathing on the screen. When he stops breathing, the light intensity decreases to zero (when the screen is completely dry). For each curve, the time corresponding to the moment when the evaporation is completed, which is the moment when the light intensity reaches its lowest value for the first time, is set to $t = 0$ second.

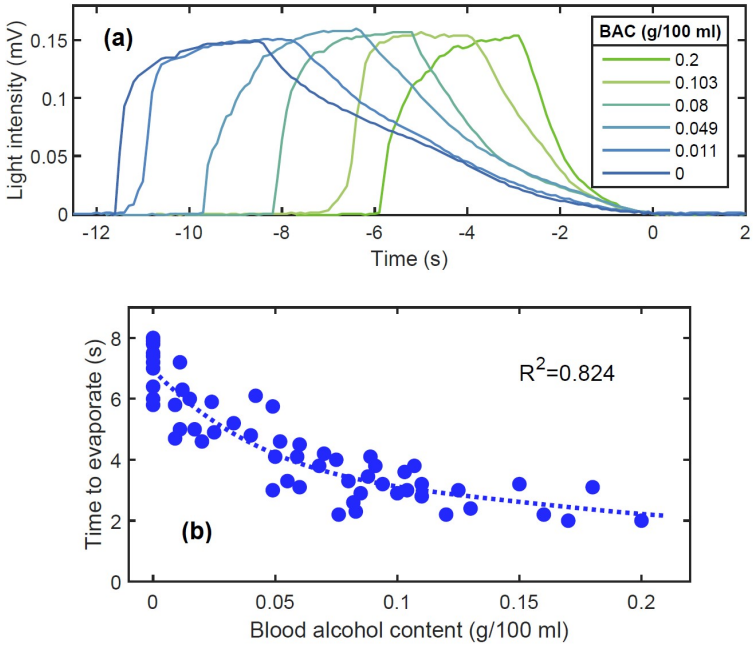

Figure 3. (a) Light intensity curves measured at the photodiode for different BACs. (b) Good correlation ($R^2 = 0.824$) between the breath evaporation time and the BAC in laboratory environment.

A water droplet can evaporate twice as fast with 20% of alcohol compared to without alcohol, depending on humidity and ambient temperature [15]. However, the rate of evaporation is not linear as a function of the alcohol concentration, due to surface tension effects. Note that the breath vapor can contain an alcohol concentration up to 14%, which is equivalent to a BAC of 0.4 g / 100 ml. At higher concentrations, coma or death is likely [22]. In addition, the proximity of the microdroplets when the screen is fogged further complicates the dynamics of evaporation. Indeed, the more droplets nearby, the more the humidity of the ambient environment increases, which decreases the rate of evaporation. This is the reason why the middle of a fogged surface remains present longer than the microdroplets located at the edges, as shown in Fig. 1 (a). It is therefore very difficult to analytically analyze the evaporation, and thus the light intensity curve measured by the detector of our breathalyzer presented in Fig. 2. A very simple parameter to analyze is the time it takes for the microdroplets to evaporate completely. The time taken for the light intensity to go from 0.12 mV to 0 (the moment when the light intensity reaches its lowest value for the first time) was used. Fig. 3 (b) shows the evaporation time as a function of the BAC measured with the commercial breathalyzer APC-90.

The coefficient of determination obtained for the n = 57 measurements compared to the best polynomial fit (dotted curve) is $R^2 = 0.824$, which demonstrates a good correlation between the measurements of our prototype and the actual BAC. The standard deviation of the BAC measured with the prototype is $\sigma = 0.037$ g / 100 ml, which is far from the precision of the APC-90, which is 0.005 g / 100 ml. A device with a precision weaker than 0.02 g / 100 ml could probably only be useful as alcohol interlock, for detecting whether the user is under the influence of alcohol or not. Note that

this latter function is becoming commonplace for access control to restricted areas, such as nuclear power plants, process industry, and mining premises [6].

4.2. Real-world tests

The ultimate goal is to design an accurate breathalyzer functional in real-world environments. To identify all the parameters that affect the measurement of our optical breathalyzer, tests were carried out during festive events. 140 measurements were carried out on 36 volunteers during three festive evenings, two in a house (Fig. 4, black markers) and the other in an indoor public place (Fig. 4, blue markers). Fig. 4 shows the evaporation time measured with our prototype as a function of the BAC measured with the APC-90. By analyzing the 140 evaporation curves as a function of time (similar to those in Fig. 3), several parameters and conditions affecting the measurements were identified. They are listed below with a discussion of their effects and possible solutions to take into account in the measurements. We hope to use these parameters and a large data set acquired in the next years in a deep neural network (DNN) training process to improve the accuracy of our breathalyzer using a machine learning approach.

4.2.1. Breathing condition

The opening of the mouth, the distance to the screen, the strength and duration of the breath are parameters that can influence the number of microdroplets as well as their combination to produce larger droplets, thus affecting the dynamics of evaporation. The use of a mechanical mechanism capable of normalizing measurements, as implemented in commercially available breathalyzers, could be used. However, the original goal of not having to carry additional items would not be achieved.

The number of microdroplets directly affects the maximum measured light intensity as well as the evaporation time. For example, one of the volunteers was not able to breath strong and long enough to fog an area large enough to obtain a maximum light intensity comparable to a normal measurement. Note that the volunteer was also unable to operate the APC-90, due to its shortness of breath. This situation may simply be canceled and a message on the screen would explain that a longer breath is required. Nevertheless, in addition to the maximum light intensity, information from the signature of the curve during the breath can be obtained. The duration of the breath can be measured between the point where the curve starts to increase and the point where the curve starts to decrease exponentially. Moreover, the initial slope provides information on the strength of the breath. Considering these data, the atypical situations could be identified and compared with each other. The situations where the initial slope, the maximum intensity or the duration of the breath is the lowest are denoted by black (house) and blue (public place) empty squares in Fig. 4. Clearly, these conditions have the effect of reducing the evaporation time.

When there is a large amount of water coming from the breath reaching the screen, the microdroplets can combine. Since it is only the edges of the droplets that allow light to reach the detector, a large droplet produces a smaller light intensity than several small droplets measured at the detector. This situation is easily detectable on the curve of light intensity as a function of time. When the light intensity decreases during evaporation, there is a moment when the light intensity stops decreasing (and can even increase). By analyzing images taken under a microscope as a function of time, we confirmed that this moment corresponds to the separation of the microdroplets. The cases in which the microdroplets are combined are represented by empty black triangles (house) and empty blue circles (public place) in Fig. 4. Clearly, the combination of microdroplets has the effect of increasing the evaporation time.

Periodic peaks are sometimes present in the light intensity curve. The intensity of these peaks is inversely proportional to the distance between the volunteer's face and the screen. Indeed, smartphones are equipped with a source and a detector to measure the distance of objects in front of the screen [23,24]. It is this detector that turns off the display and the touch-screen functions when the user approaches the phone from his ear while answering a phone call. Since this source does not emit visible light, a simple filter placed in front of the breathalyzer detector would remove these

Preprints (www.preprints.org) | NOT PEER-REVIEWED | Posted: 19 April 2021 doi:10.20944/preprints202104.0502.v1

peaks. However, the duration and intensity of these peaks provides information on the position of the volunteer's face which could be used in the analysis of the evaporation curve.

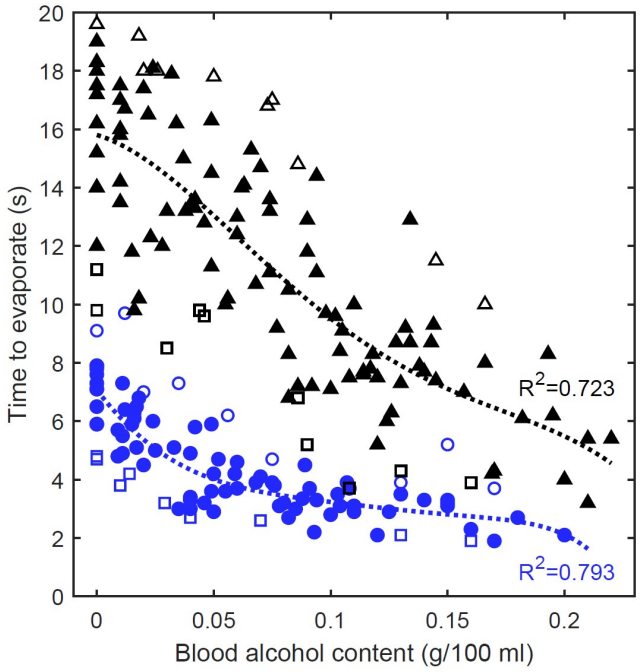

Figure 4. Utilization of our breathalyzer in real-world environment. The weak correlation between the breath evaporation time and the BAC is greatly improved by considering a few measurable parameters. Blue markers: humidity of 0.32. Black markers: humidity of 0.53. Empty markers: detected anomalies.

4.2.2. Ambient conditions

Humidity, temperature, wind and ambient light can affect the measurements. Wind should be avoided as it results in faster evaporation of the microdroplets. The breathalyzer should therefore be used indoors or in windless conditions. To maximize the accuracy of the breathalyzer, the ambient humidity and temperature should be known, which can be obtained with the sensors of recent smartphones [23,24] or entered by the user. We observed that the ambient light produced noise in the measurements. In fact, the ambient light can reach the detector due to the diffusion in the glass screen. The breathalyzer response can be analyzed considering the light noise measured and compared with a reference with the same light noise. Restricting the use of the breathalyzer in the dark could also solves the problem. Adding an electronic filter that only keeps the display's refresh rate frequency could discriminate it from other light sources such as sunlight. Adding an optical filter in front of the detector, allowing only the highest intensity of the display spectrum to pass, would also improve the results. Finally, the screen should be properly cleaned before every test. Dirt on the screen produces a constant light noise on the detector (due to the same principle as with microdroplets).

Under non-optimal ambient conditions (judged by the user or detected by the smartphone), a measurement of the breathalyzer performed with the breath from a sober person could serve as a reference to calibrate the device and improve the accuracy of the next test.

4.2.3. Post-processed results

As shown in Fig. 4, the breathalyzer is not accurate in real-world situations without post processing the data (R^2 = 0,170 for n = 140). In fact, an evaporation time of over 10 seconds can be obtained from a BAC of 0.15 while an evaporation time of 5 seconds can be obtained from a sober person. However, considering a few simple parameters, the correlation can be greatly improved. By comparing the values in Fig. 4 with the same ambient humidity, the coefficient of determination increases to R^2 = 0.617 in the public place (blue markers) and R^2 = 0.614 in the house (black markers). The humidity was 0.32 in the public place and 0.53 in the house, measured with a household hygrometer (Bios Weather). In addition, by simply discarding atypical data, as

previously discussed (empty markers in Fig. 4), the coefficient of determination increases to $R^2 = 0.793$ in the public place and $R^2 = 0.723$ in the house, which is evidencing the room for improvement that could be provided by appropriate post-processing. We are currently investigating different approaches to address this issue.

5. Conclusions and future work

Our next step is to acquire a large data set of BAC optical signatures (as in Fig. 3 (a)) using our prototype in several festive events in order to train a DNN and use machine learning to obtain accurate BAC measurements. The ambient and breathing conditions discussed earlier will be used in a supervised training mode [25] in which the connection weights of the DNN are adjusted by minimizing the training loss function (difference between the actual DNN output and its desired output). Using this approach, we hope to provide a robust, ecological (no disposable parts or occasional replacement of degraded chemical sensor elements), inexpensive and discreet wearable breathalyzer that can make a real impact in the society. Finally, our contactless technology could be an interesting approach for medical diagnosis and triage at emergency medical care (or even in the street). It is common that the medical condition (head injury, stroke, heart attack, diabetes, or psychological illness) of the patient can be mistaken for alcohol intoxication. Unfortunately, state-of-the-art breathalyzers require active involvement of the patient, and expiratory volume and flow incompatible with patients' respiratory function [5,6].

Innovative applications using a smartphone as an operating medium are growing fast, demonstrating the demand for portable sensors [18,19,26-32]. The combination of these applications will hopefully someday make the smartphone a lab-at-hand.

Author Contributions: Conceptualization, Jerome Lapointe; Funding acquisition, Réal Vallée; Methodology, Jerome Lapointe, Hélène-Sarah Bécotte-Boutin, Stéphane Gagnon, Simon Levasseur, Philippe Labranche, Marc D'Auteuil, Ming-Jun Li and Réal Vallée; Software, Jerome Lapointe and Manel Abdellatif; Supervision, Réal Vallée; Writing – original draft, Jerome Lapointe and Hélène-Sarah Bécotte-Boutin; Writing – review & editing, Réal Vallée. All authors have read and agreed to the published version of the manuscript.

Funding: This research was funded by Canada First Research Excellence Fund (Sentinel North).

Acknowledgments: This research was supported by the Sentinel North program of Université Laval, made possible, in part, thanks to funding from the Canada First Research Excellence Fund.

Conflicts of Interest: The authors declare no conflict of interest.

References

1. Aseev, O.; Tuzson, B.; Looser, H.; Scheidegger, P.; Liu, C.; Morstein, C.; Niederhauser, B.; Emmenegger, L. High-precision ethanol measurement by mid-IR laser absorption spectroscopy for metrological applications. *Opt. Express* **2019,** *27*, 5314-5325.
2. Bihar, E.; Deng, Y.; Miyake, T.; Saadaoui, M.; Malliaras, G. G.; Rolandi, M. A Disposable paper breathalyzer with an alcohol sensing organic electrochemical transistor. *Sci. Rep.* **2016**, *6*, 1-6.
3. Ljungblad, J.; Hök, B.; Ekström, M. Development and evaluation of algorithms for breath alcohol screening. *Sensors* **2016**, *16*, 469.
4. Jurič, A.; Fijačko, A.; Bakulić, L.; Orešić, T.; Gmajnički, I. Evaluation of breath alcohol analysers by comparison of breath and blood alcohol concentrations. *Archives of Industrial Hygiene and Toxicology* **2018**, *69*, 69-76.
5. Jonsson, A.; Hök, B.; Andersson, L.; Hedenstierna, G. Methodology investigation of expirograms for enabling contact free breath alcohol analysis. *J. Breath Res.* **2009**, *3*, 036002.
6. Hok, B.; Pettersson, H.; Andersson, A. K.; Haasl, S.; Akerlund, P. Breath analyzer for alcolocks and screening devices. *IEEE Sens. J.* **2009**, *10*, 10-15.
7. Kim, S. Y.; Kim, J.; Cheong, W. H.; Lee, I. J.; Lee, H.; Im, H. G.; Kong, H.; Bae, B. S.; Park, J. U. Alcohol gas sensors capable of wireless detection using In2O3/Pt nanoparticles and Ag nanowires. *Sens. Actuators B Chem.* **2018**, *259*, 825-832.
8. Thungon, P. D.; Kakoti, A.; Ngashangva, L.; Goswami, P. Advances in developing rapid, reliable and portable detection systems for alcohol. *Biosens. Bioelectron.* **2017**, *97*, 83-99.

9. National Center for Statistics and Analysis. 2018 fatal motor vehicle crashes: Overview. (Traffic Safety Facts Research Note. Report No. DOT HS 812 826). Washington, DC: National Highway Traffic Safety Administration. **2019**
10. Vanlaar, W.; Robertson, R.; Marcoux, K.; Mayhew, D.; Brown, S.; Boase, P. Trends in alcohol-impaired driving in Canada. *Accid. Anal. Prev.*. **2012**, *48*, 297-302.
11. Ramchandani, V. A.; Kwo, P. Y.; Li, T. K. Effect of food and food composition on alcohol elimination rates in healthy men and women. *J. Clin. Pharmacol*. **2001**, *41*, 1345-1350.
12. Cromer, J. R.; Cromer, J. A.; Maruff, P.; Snyder, P. J. Perception of alcohol intoxication shows acute tolerance while executive functions remain impaired. *Exp. Clin. Psychopharmacol*. **2010**, *18*, 329.
13. Elder, R. W.; Voas, R.; Beirness, D.; Shults, R. A.; Sleet, D. A.; Nichols, J. L.; Compton, R. Effectiveness of ignition interlocks for preventing alcohol-impaired driving and alcohol-related crashes: a Community Guide systematic review. Am. J. Prev. Med. **2011**, *40*, 362-376.
14. Min, A.; Lee, D.; Shih, P. C. Potentials of Smart Breathalyzer: Interventions for Excessive Drinking Among College Students. In *Transforming Digital Worlds. iConference 2018. Lecture Notes in Computer Science*. Chowdhury G., McLeod J., Gillet V., Willett P., Eds.; Springer, Cham. 2018, Volume 10766, pp. 195-206.
15. Liu, C.; Bonaccurso, E.; Butt, H. J. Evaporation of sessile water/ethanol drops in a controlled environment. *Phys. Chem. Chem. Phys.* **2008**, *10*, 7150-7157.
16. Marcuse, D. Launching light into fiber cores from sources located in the cladding. *J. Light. Technol.* **1988**, *6*, 1273-1279.
17. Snyder, A. W.; Love, J. *Optical waveguide theory*. Springer Science & Business Media. 2012.
18. Lapointe, J.; Gagné, M.; Li, M. J.; Kashyap, R. Making smart phones smarter with photonics. *Opt. Express.* **2014**, *22*, 15473-15483.
19. Lapointe, J.; Parent, F.; de Lima Filho, E. S.; Loranger, S.; Kashyap, R. Toward the integration of optical sensors in smartphone screens using femtosecond laser writing. *Opt. Lett.* **2015**, *40*, 5654-5657.
20. Lapointe, J.; Kashyap, R. A simple technique to overcome self-focusing, filamentation, supercontinuum generation, aberrations, depth dependence and waveguide interface roughness using fs laser processing. *Sci. Rep.* **2017**, *7*, 1-13.
21. Lapointe, J.; Bérubé, J. P.; Ledemi, Y.; Dupont, A.; Fortin, V.; Messaddeq, Y.; Vallée, R. Nonlinear increase, invisibility, and sign inversion of a localized fs-laser-induced refractive index change in crystals and glasses. *Light Sci. Appl.* **2020**, *9*, 1-12.
22. Dubowski, K. M. Alcohol determination in the clinical laboratory. *Am. J. Clin. Pathol*. **1980**, *74*, 747-750.
23. Majumder, S.; Deen, M. J. Smartphone sensors for health monitoring and diagnosis. *Sensors* **2019**, *19*, 2164.
24. Su, X.; Tong, H.; Ji, P. Activity recognition with smartphone sensors. *Tsinghua Sci. Technol*. **2014**, *19*, 235-249.
25. LeCun, Y.; Bengio, Y.; Hinton, G. (2015). Deep learning. *Nature*. **2015**, *521*, 436-444.
26. Hossain, M. A.; Canning, J.; Yu, Z;, Ast, S.; Rutledge, P. J.; Wong, J. K. H.; Jamalipour, A.; Crossley, M. J. Time-resolved and temperature tuneable measurements of fluorescent intensity using a smartphone fluorimeter. *Analyst* **2017**, *142*, 1953-1961.
27. Stieger, S.; Reips, U. D. Well-being, smartphone sensors, and data from open-access databases: A mobile experience sampling study. *Field Methods* **2019**, *31*, 277-291.
28. Hossain, M. A.; Canning, J.; Yu, Z. Fluorescence-based determination of olive oil quality using an endoscopic smart mobile spectrofluorimeter. *IEEE Sens. J.* **2019**, *20*, 4156-4163.
29. Lapointe, J.; Bérubé, J. P.; Ledemi, Y.; Dupont, A.; Fortin, V.; Messaddeq, Y.; Vallée, R. Miniaturized and invisible laser-inscribed photonic circuits. Photonics North, Niagara Falls, Canada, 2020, May.
30. Crocombe, R. A. Portable spectroscopy. *Appl. Spectrosc.* **2018**, *72*, 1701-1751.
31. Abasi, S.; Minaei, S.; Jamshidi, B.; Fathi, D. Development of an Optical Smart Portable Instrument for Fruit Quality Detection. *IEEE Trans. Instrum. Meas.* **2020**, *70*, 1-9.
32. Nelis, J.; Elliott, C.; Campbell, K. "The Smartphone's Guide to the Galaxy": In Situ Analysis in Space. *Biosensors* **2018**, *8*, 96.